Synthesis, photophysical and electrochemical properties of a blue emitter with binaphthalene and carbazole units

Lixia Guo, Xiaoju Wang, Liheng Feng

PII: S1386-1425(18)30379-2
DOI: doi:10.1016/j.saa.2018.04.067
Reference: SAA 16052

To appear in: *Spectrochimica Acta Part A: Molecular and Biomolecular Spectroscopy*

Received date: 28 July 2017
Revised date: 17 April 2018
Accepted date: 29 April 2018

Please cite this article as: Lixia Guo, Xiaoju Wang, Liheng Feng , Synthesis, photophysical and electrochemical properties of a blue emitter with binaphthalene and carbazole units. The address for the corresponding author was captured as affiliation for all authors. Please check if appropriate. Saa(2017), doi:10.1016/j.saa.2018.04.067

Synthesis, photophysical and electrochemical properties of a blue emitter with binaphthalene and carbazole units

Lixia Guo[a1], Xiaoju Wang[b1], Liheng Feng[a*]

[a]*School of Chemistry and Chemical Engineering, Shanxi University, Taiyuan, 030006, P.R. China.*
[b]*Institute of Molecular Science, Chemical Biology and Molecular Engineering, Laboratory of Education Ministry, Shanxi University, Taiyuan 030006, PR China;*

Abstract: A blue emitter, 3,3'-(2,2'-dimethoxy-[1,1'-binaphthalene]-6,6'-diyl)bis(9-benzyl-9H-carbazole), was synthesized by Suzuki coupling reaction. The photophysical properties of the emitter in solution were firstly investigated by UV-Vis absorption and fluorescence emission techniques. The results indicate that the emitter has excellent optical and electron transfer properties. The maximum absorption and emission peaks of the emitter are 302 nm and 406 nm with 67.4 % fluorescence quantum yield in chloroform, respectively. Thermal stability study reveals that the emitter has a good thermal stability (Td>330 °C, Tg>160 °C). Electrochemical Redox properties of the emitters were measured by cyclic voltammetry, and the energy gaps of highest occupied molecular orbital and the lowest unoccupied molecular orbital levels are in good agreement with the results of theoretical calculation. Furthermore, the multilayer electrochemcial device with the emitter was fabricated and its properties were explored. The wavelength of electroluminescence for the device with this emitter locates at 428 nm. These results indicate the emitter as a deep blue-emitting material has promising application in organic light-emitting diode devices.

Keywords: Blue emitter, Property, Suzuki reaction, Naphthalene, Carbazole

---

[*] E-mail address: lhfeng@sxu.edu.cn (L. Feng); Tel.:+86 351 7010904; Fax: +86 351 7011688.
[1]The authors of Lixia Guo and Xiaoju Wang contributed equally to this work.

1. Introduction

Since the discovery of organic light emitting diodes (OLEDs), it has drawn considerable attention because of their delocalized electronic structures, large π-conjugated backbone, easy availability, high efficiency and the potential applications in full-color flat panel displays and solid state lighting [1-5]. In the performance of the devices, light-emitting materials play an essential role. So far, researchers have made every effort to design and prepare a wide variety of light-emitting materials [6-21]. The vast majority of luminescent materials used in OLEDs are organic small molecules, oligomers, metal complexes and polymers containing a variety of aromatic and π-conjugated units [22-25]. Among various OLEDs, the blue-emitting material is desired, especially the deep blue emitters. Therefore, there is an increasing need to develop stable, high-intensity, efficient deep blue emitters for OLEDs application.

Carbazole is a typical hole-transporting group. The materials including carbazole units have high temperature resistance and strongly intense luminescence. Based on these properties, when introducing carbazole group to the core structure of OLED emitter, the morphological and thermal stabilities of this material can be vastly improved [26-28]. Additionally, the materials with carbazole display stronger brightness and higher stability [29]. Carbazole and its derivations have been frequently used to design novel host materials in OLED owing to their high triplet energy level and low oxidation potential [30-34]. Due to its ten carbon atoms ring and delocalization conjugated bond, naphthalene is quite stable and usually uses as a blue emitter. The wavelength of naphthalene always takes place red-shift by conjugating with other organic molecules. Furthermore, polycyclic aromatic hydrocarbons exhibited intense fluorescence in many situations because of their rigid planar [35]. It was also used in manufacturing dyes, water purification, fluorescent probe and other organic compounds [36-40]. As we all know that the balance of the transport of hole and injection of electron is imperative for obtaining an excellent OLEDs device. So, it is necessary to obtain an excellent OLED device by combining the electron-transfer group and hole-transfer group in the same compound [41-44].

In view of the above idea, in here, we reported a proficient conjugated material containing carbazole and naphthalene units (MNBC) as an emitter in the OLED device. In this emitter, carbazole unit is a hole-transfer group. Naphthalene group not only acts as electron-transfer role but also is a supplier of blue light emission. Through UV-Vis absorption and fluorescence emission techniques, the photophysical properties of the emitter were investigated. The thermostability and electrochemical property of MNBC also were studied. In order to develop the application, the OLED device with the material as an emitter was fabricated. These results indicate that the emitter is a promising and desired deep blue-emitting material in organic light-emitting diodes (OLEDs).

2. Experimental

2.1 Materials and instruments

Unless otherwise stated, all chemical reagents were obtained from commercial supplier and were used without further purification. Benzyl bromide, 9H-carbazole, N-Bromosuccinimide (NBS), toluene and dibromine were obtained by Aladdin (Tianjin, China). Bis(pinacolato)diboron, (*R*)-2,2'-dimethoxy-1,1'-binaphthalene, $Pd(PPh_3)_4$ and $Pd(dppf)Cl_2$ were all purchased from Aldrich (Steinheim, Germany). Bruker ARX400 spectrometer was used for measuring ^1H NMR and ^{13}C NMR of products with chemical shifts reported as ppm (TMS as an internal standard). Mass spectra (MS) were acquired on an Agilent 6510 Q-TOF LC/MS instrument (Agilent

Technologies, Palo Alto, CA) with an electrospray ionization (ESI) source. Elemental analyses was measured on a EuroVector EA3000 elemental analyzer. The UV-Vis absorption and fluorescence emission spectra were reported on a HITACHI UH5300 and F-4600 spectrophotometers, respectively. The excitation and emission slit widths were both 5.0 nm. The glass transition temperature of the emitter was determined by DSC using a DSC-Q10 instrument under nitrogen atmosphere. The decomposition temperature corresponding to 5 % weight loss was detected by Perkine Elmer Pyris 1 TGA thermal analyzer. Cyclic voltammetry (CV) measurement was determined on three-electrode AUTOLAB (model PGSTAT30) workstation in a solution of Bu_4NClO_4 (0.1 M) in acetonitrile at a scan rate of 50 mV/s at room temperature.

2.2 Synthesis of monomers and emitter MNBC

2.2.1 Synthesis of monomer1 and monomer 2

The 9-benzyl-3-bromo-9H-carbazole (monomer 1) and 2,2'-(2,2'-dimethoxy-[1,1'-binaphthalene]-6,6'-diyl)bis(4,4,5,5-tetramethyl-1,3,2-dioxaborolane) (monomer 2) were prepared according to our previous reported methods [45,46]. The characterization data were listed as follows: *9-benzyl-3-bromo-9H-carbazole* (monomer 1): ^{1}H NMR ($CDCl_3$, 400 MHz) δ 8.302 (d, *J*=12.8 Hz, 1H), 8.198 (s, 1H), 7.854 (t, *J*=12.8, 9.6 Hz, 1H), 7.460-7.364 (m, 3H), 7.358-7.221 (m, 4H), 7.162 (t, *J*=10.8, 9.6 Hz, 2H), 5.513 (s, 2H); ^{13}C NMR ($CDCl_3$, 100 MHz) δ 142.84, 140.66, 135.94, 132.43, 127.57, 127.38, 126.32, 125.91, 123.38, 120.63, 119.54, 118.99, 102.45, 44.48; EI-MS for $C_{19}H_{14}BrN$ (m/z) 335.2 [M^+], 337.1 [M^++2].

2,2'-(2,2'-dimethoxy-[1,1'-binaphthalene]-6,6'-diyl)bis(4,4,5,5-tetramethyl-1,3,2-dioxaborolane) (monomer 2): ^{1}H NMR (*d*-$CDCl_3$, 400 MHz) δ 8.421 (s, 2H), 8.053 (d, *J*=9.2 Hz, 2H), 7.586 (d, *J*=7.6 Hz, 2H), 7.468 (d, *J*=9.2 Hz, 2H), 7.102 (d, *J*=8.4 Hz, 2H), 3.759 (s, 6H), 1.382 (s, 24H); ^{13}C NMR (*d*-DMSO, 100 MHz) δ 25.02, 56.69, 83.69, 99.99, 113.93, 119.30, 124.30, 128.59, 130.33, 130.83, 135.72, 136.51, 155.92; EI-MS for $C_{34}H_{40}B_2O_6$ (m/z) 567.2 [M^++2], 566.1 [M^++1], 565.4 [M^+].

2.2.2 Synthesis of 3,3'-(2,2'-dimethoxy-[1,1'-binaphthalene]-6,6'-diyl)bis(9-benzyl-9H-carbazole)(MNBC)

A mixture of 2.83 g 2,2'-(2,2'-dimethoxy-[1,1'-binaphthalene]-6,6'-diyl)bis-(4,4,5,5-tetramethyl-1,3,2-dioxaborolane)1,6-dibromopyrene (0.5 mol), 3.36 g 9-benzyl-3-bromo-9H-carbazole (1.0 mol) in toluene (30.0 mL) and 2.0 M Na_2CO_3 (10.0 mL) was stirred for 30 min at room temperature under nitrogen atmosphere. Then, $Pd(PPh_3)_4$ (0.1 g) catalyst was quickly added to the suspension and heated to 110 °C for 48 h under nitrogen atmosphere. After cooling it to room temperature, the solvent was removed under reduced pressure. The crude product was obtained through extraction with dichloromethane, drying with anhydrous sodium sulfate and desolventizing. And then, it purified by column chromatography on silica gel with dichloromethane/petroleum ether (1/2, v/v) as the eluant to afford MNBC as tephrosious solids (1.58 g 38.4 %). ^{1}H NMR ($CDCl_3$, 400 MHz) δ 8.435 (d, *J*=7.6 Hz, 2H), 8.195 (t, *J*=4.8, 6.6 Hz, 4H), 8.114 (t, *J*=9.6, 7.6 Hz, 2H), 7.790 (t, *J*=4.8, 4.4 Hz, 2H), 7.762 (t, *J*=4.8, 6.4Hz, 2H), 77.554 (d, *J*=9.6Hz, 2H), 7.478-7.403 (m, 6H), 7.376-7.270 (m, 8H), 7.199-7.179 (d, *J*=8.0 Hz, 6H), 5.562 (s, 4H), 3.842 (s, 6H); ^{13}C NMR ($CDCl_3$, 100 MHz) δ 154.94, 141.11, 140.07, 137.13, 132.88, 132.82, 129.69, 129.62, 128.82, 127.51, 126.66, 126.44, 125.86, 123.59, 123.19, 120.49, 119.59, 119.33, 118.99, 114.68, 109.16, 105.04, 57.03, 46.71; EI-MS for $C_{60}H_{44}N_2O_2$ (m/z) 824.2 [M^+]. Element Analysis for $C_{60}H_{44}N_2O_2$ (Mol. Wt.: 825.02) calcd.: C, 87.35; H, 5.38; N, 3.40; found: C, 86.88; H, 5.43; N, 3.32.

2.3 Fluorescence and UV-Vis measurements

The stock solution of compound MNBC was 1.0×10^{-2} mol/L in $CHCl_3$. Corresponding, the stock solutions of N,N-dimethylaniline (DMA), dimethylterephthalate(DMTP) and C_{60} were all 1.0×10^{-2} mol/L in organic solvents, respectively. Through the dilution method, various working solutions were prepared. The working solution (1.0×10^{-5} mol/L) was placed in a quartz cuvette with 1 cm path, and the total volume of it was 2.0 mL. The stock solutions of DMA, DMTP and C_{60} were added to the MNBC working solution, respectively. After shaking for 30 s, the new spectra were measured. The volume added of DMA, DMTP and C_{60} did not exceed 3% of the total. All of the experiments were performed at barometric pressure and room temperature.

2.3 Device fabrication

The vacuum-deposition technique was used to fabricate the multilayer OLEDs. In the device, ITO layer acted as anode and organic layers was fabricated by high-vacuum (5×10^{4} Pa) thermal evaporation onto a glass (3 cm×3 cm) substrate percolated. Poly(3,4-ethylenedioxythiophene):poly(styrenesulfonate) (PEDOT: PSS) served as the hole-transfer layer (HTL). The electron-blocking layer was 4,4-bis(*N*-carbazolyl)-1,10-biphenyl (CBP). The emitter MNBC acted as an emitting layer. The electron-transport layer (ETL) was 1,3,5-tris(*N*-phbenylbenzimidazol-2-yl) benzene (TBPI). The cathode was the LiF/Al. All organic layers were placed according the prescribed order. Thermal deposition rates for organic materials, LiF and Al were 0.5 $Å\cdot s^{-1}$, $0.5\cdot Å\ s^{-1}$and 1.0 $Å\cdot s^{-1}$, respectively. The active area of the device was 9 mm^2. The electroluminescent spectra were reported on a Hitachi MPF-4 fluorescence spectrometer. The voltage-current density characteristic of OLEDs was obtained on Keithley 2400 Source Meter. The characterization of luminance-voltage was measured with a 3645 DC power supply combined with a 1980 A spot photometer and the data was recorded simultaneously. All measurements were conducted at room temperature.

3. Results and discussion

3.1 Synthesis of MNBC

The emitter MNBC was prepared by Suzuki coupling reaction of monomer 1 and monomer 2 in the presence of palladium catalyst with 38.4 % yield. Carbazole units in monomer 1 acts as a hole transport group, and naphthalene unit in monomer 2 is an electron transport group. The detail synthetic routes for monomers and MNBC were described in **Scheme 1**. The two monomers were synthesized by our previously reported methods. The structures of monomers and MNBC were characterized and verified by ^{1}H NMR, ^{13}C NMR, Mass spectra (MS) and elemental analysis (EA). The MNBC has a poor solubility in routine solvents (such as ethanol, acetone, ethyl acetate, etc.) because of its larger rigid conjugated structure.

3.2 Photophysical properties of MNBC

The photophysical properties of MNBC in $CHCl_3$ were studied by UV-Vis absorption and fluorescence emission spectra (**Fig.1**). As can be seen from **Fig. 1**, the two major absorption peaks of compound MNBC locate at 249 nm and 302 nm, which mainly comes from the characteristic of vibronic pattern for the carbazole groups, respectively. Based on the maximum absorption wavelength, the optical energy band gap (4.10 eV) of MNBC was obtained by the empirical equation [$E_g=1240/\lambda_{abs}$]. Accordingly, the fluorescence emission peak of MNBC locates at 388 nm with a shoulder peak in 406 nm. The fluorescent quantum yield (Φ) of MNBC is 67.4 % in chloroform with quinine sulfate in 0.10 M sulfuric acid as the reference. In order to investigate the solvent effect of MNBC, the fluorescence spectra of MNBC in different organic solvents were investigated and listed in ***Fig.S1***. From ***Fig.S1***, the maximum emission wavelength (λ_{em}) of MNBC occurred gradually red-shifted (30-50 nm) with increase of solvent polarity. Similar, the half bandwidth ($\lambda_{em½}$) also had a slight increase with the increase of the solvent polarity. Additionally, the electron transfer property of MNBC in solution also was studied. In this aspect, the interactions of MNBC with electron donor (DMA), electron acceptor (DMTP) and C_{60} were obtained by the titration method, respectively. These results are summarized in ***Fig.S2a-d.*** These data indicate that the MNBC has a good electronic transmission capacity, which is beneficial for OLED fabrication.

3.3 Thermal properties of MNBC

Thermal property is a powerful parameter for testing the OLED materials. The thermal properties of MNBC were tested by using differential scanning calorimeter (DSC) with a heating rate of 5 °C/min under nitrogen atmosphere. The test exhibits that MNBC shows good thermostability because of its large molecular masses and rigid structure. The decomposition temperature (Td, 5 % weight loss) of MNBC is 181ºC (**Fig.2**). Accordingly, the glass transition temperatures (Tg) of MNBC is 152 ºC. The high thermal stability of MNBC will contribute to the device performance (longevity).

3.4 Electrochemical property and theoretical calculation

The electrochemical property is also a way to evaluate the performance of the material. Cyclic voltammograms (CV) were performed with a voltammetric analyzer (CHI660E) with saturated calomel electrode as the reference electrode. The electrochemical experiment was carried out in the supporting electrolyte under nitrogen atmosphere at room temperature. The supporting electrolyte was a solution of acetonitrile containing 0.1 M tetrabutylammonium perchlorate (n-Bu_4NClO_4). The concentration of MNBC was 1.0 mM. As shown in **Fig.3**, the electrochemical window possesses a reversible reduction peak. The reversible oxidation peak is about +0.38 eV and the reversible reduction peak is about -1.25eV, which mainly attributes to the oxidation of the carbazole groups and electron injection into the vacant naphthalene. From the empirical equation [HOMO= -(Eox+4.5+0.24)eV], we can get the value of the HOMO energy level is -5.12 eV, which indicates the electron distribution mainly comes from the carbazole moiety. These results further demonstrate that this MNBC can be used as an efficient hole-injection materials. From the maximum absorption peak and empirical equation [E_g=1240/λ_{abs}], we can obtain the energy gap (Eg) of the MNBC is 4.10 eV. Accordingly, the LUMO energy level of MNBC is -0.90 eV, which is obtained by the difference between E_{HOMO} and E_g.

In order to verify the experiment results, the energy levels of MNBC in the acetonitrile solvent were calculated by using density functional theory (DFT) method with the basis sets 6-31G(d) on Gaussian 09 software [47-48]. The geometries and electron density distributions of the HOMO (highest occupied molecular orbital) and LUMO (lowest unoccupied molecular orbital) energy levels of MNBC were described in **Fig.3**. Based on the conversion relation (1 a.u.= 27.2114 eV)[49], the value of E_{HOMO} (-5.20 eV) was obtained by the calculated result of E_{HOMO} (-0.19117 a.u.). And, electron density in HOMO state locates on the whole conjugated skeleton. Accordingly, E_{LUMO} is calculate as -1.19 eV. The electron density in LUMO state locates mainly on the naphthalene moiety. The results are similar to those in electrochemical. Besides, the Mulliken charges and their distribution of MNBC were also studied in ***Fig.S3***. As shown in ***Fig.S3***, the large negative values in the BMNC molecules are N86, N58, O25, and O26, respectively. This is due to the electron-withdrawing ability of these atoms. Correspondingly, the C atoms attached to these atoms are large positive values. Regardless of C4 and C10, C82 and C48 or C85 and C51, the positions of these atoms are corresponding and their values are similar, which is attributed to the higher symmetry of the structure of BMNC. The dipole moment of MNBC is 1.5738 debye. Furthermore, the excited-state absorption spectrum of MNBC in chloroform was calculated by TDDFT, with the hybrid B3LYP functional and the 6-31G(d) basis set. The absorption spectrum calculated by theoretical was shown in ***Fig.S4***. The absorption wavelength of the compound in chloroform is located at 310 nm, which matches with the result by UV-Vis spectrophotometer.

3.5 Electroluminescence Devices

In order to evaluate MNBC as an emitter in OLEDs, a multilayers non-doped device: ITO/PEDOT:PSS(40nm)/MNBC(21nm)/TPBI(40nm)/LiF(1nm)/Al (200nm) was fabricated (**Fig.4a**). The electroluminescence (EL) spectra of the device were determined under different voltages and listed in **Fig.4b**. From **Fig.4b**, we can find that the emission peak of the device locates at 428 nm and the wavelength does not change with the increase of voltages, which indicates the MNBC can emit a deep blue light and has a good stability in OLED device. The voltage-luminance and voltage-current density curves of the device were listed in the **Fig. 4c** and **4d**, respectively. From these data, we can find the turn-on voltage, maximum luminance, maximum current efficiency and maximum power efficiency of the device are 5.5 V, 535 cd m^{-2} (at 15 V), 0.659 cd A^{-1} (at 6 V) and 0.345 l $m\cdot W^{-1}$(at 6 V), respectively. Owing to the experiments carry out under ordinary laboratory conditions and the experimental dates were not reflected the optimized devices, by changing the layer thickness, optimizing the process conditions, we trust the performance of the device will be improved.

4. Conclusion

In conclusion, we have successfully designed and synthesized a novel deep blue-emitting OLED material. The studies of photophysical properties show that the MNBC can emit a deep blue light with a higher quantum yield in solution. The electrochemical and thermal properties of MNBC also were investigated carefully. The results indicates that this compound MNBC processes good π-electron delocalization and conjugation features, high thermal stability and glass transition temperature, excellent optical and electrical characteristics. The device with the MNBC emitter was fabricated and emitted deep blue light. Further photoelectric device tests of the emitter are in progress and reported subsequently.

Acknowledgment

The work described in this paper was supported by the National Nature Science Foundation (No.21601111, 21571116 and 21371110), Youth Science Foundation of Shanxi Province (No.201601D021054), Scientific and Technologial Innovation Programs of Higher Education Institutions in Shanxi (No. 2017108), Program for the Outstanding Innovative Teams of Higher Learning Institutions of Shanxi (No. 2017-07), and SanJin Scholars Support Plan under Special Funding (No. 2017-06). We also thank the Scientific Instrument Cente of Shanxi University for assistances during the characterizations of the compounds.

Appendix. Supplementary data

Other fluorescence spectroscopy (PDF) associated with this article can be found in the online version, at doi:

References

[1] Tang CW, Vanslyke SA. Organic electroluminescent diodes. Appl Phys Lett 1987; 51: 913-5.

[2] Grimsdale AC, Chan KL, Martin RE, Jokisz PG, Holmes AB. Synthesis of light-emitting conjugated polymers for applications in electroluminescent devices. Chem Rev 2009; 109: 897-1091.

[3] Li W, Li JY, Wang F, Gao Z, Zhang SF. Universal host materials for high-Efficiency phosphorescent and delayed-fluorescence OLEDs. ACS Appl Mater Interfaces 2015; 7: 26206-16.

[4] Tavgeniene D, Liu L, Krucaite G, Volyniuk D, Grazulevicius JV, Xie Z, et al. Phenylvinyl-substituted carbazole twin compounds as efficient materials for the charge-transporting layers of OLED devices. J Electron Mater 2015; 44: 4006-11.

[5] Liu W, Zheng CJ, Wang K, Chen Z, Chen DY, Li F, et al. Novel carbazol-pyridine-carbonitrile derivative as excellent blue thermally activated delayed fluorescence emitter for highly efficient organic light-emitting devices. ACS Appl Mater Interfaces 2015; 7: 18930-6.

[6] Li W, Li JY, Liu D, Jin Q. Simple bipolar host materials for high-efficiency blue, green, and white phosphorescence OLEDs. ACS Appl Mater Interfaces 2016; 8: 22382-91.

[7] Thiery S, Tondelier D, Geffroy B, Jacques E, Robin M, Metivier R, et al. Spirobifluorene-2,7-dicarbazole-4'-phosphine Oxide as Host for High-Performance Single-Layer Green Phosphorescent OLED Devices. Org Lett 2015; 17: 4682-5.

[8] Chu X, Guan M, Niu LT, Zeng YP, Li YY, Zhang Y, et al. Fast responsive and highly efficient optical upconverter based on phosphorescent OLED. ACS Appl Mater Interfaces 2014; 6: 19011-6.

[9] Steiner F, Bange S, Vogelsang J, Lupton JM. Spontaneous fluctuations of transition dipole moment orientation in OLED triplet emitters. J Phys Chem Lett 2015; 6: 999-1004.

[10] Jou JH, Sahoo S, Kumar S, Yu HH, Fang PH, Singh M, et al. A wet- and dry-process feasible carbazole type host for highly efficient phosphorescent OLEDs. J Mater Chem C 2015; 3: 12297-307.

[11] Chen CH, Hsu LC, Rajamalli P, Chang YW, Wu FI, Liao CY, et al. Highly efficient orange and deep-red organic light emitting diodes with long operational lifetimes using carbazole–quinoline based bipolar host materials. J Mater Chem C 2014; 2: 6183-91.

[12] Shi HP, Xin DH, Gu XG, Zhang PF, Peng HR, Chen SM, et al. The synthesis of novel AIE emitters with the triphenylethene-carbazole skeleton and para-/meta-substituted arylboron groups and their application in efficient non-doped OLEDs. J Mater Chem C 2016; 4: 1228-37.

[13] Cheng SH, Hung WY, Cheng MH, Chen HF, Lee GH, Chung CL, et al. Highly twisted carbazole-oxadiazole hybrids as universal bipolar hosts for high efficiency OLEDs. Adv Electron Mater 2016; 2: 1500241.

[14] Ameen S, Lee SB, Yoon SC, Lee J, Lee C. Diphenylaminocarbazoles by 1,8-functionalization of carbazole: Materials and application to phosphorescent organic light-emitting diodes. Dyes Pigm 2016; 124: 35-44.

[15] Hellerich ES, Manna E, Heise R, Biswas R, Shinar R, Shinar J. Deep blue/ultraviolet microcavity OLEDs based on solution-processed PVK:CBP blends. Org Electron 2015; 24: 246-53.

[16] Huang Y, Du X, Tao S, Yang X, Zheng CJ, Zhang X, et al. High efficiency non-doped deep-blue and fluorescent/phosphorescent white organic light-emitting diodes based on an anthracene derivative. Synth Met 2015; 203: 49-53.

[17] Lee SB, Park SN, Kim C, Lee HW, Lee HW, Kim YK et al. Synthesis and electroluminescent properties of 9,10-diphenylanthracene containing 9H-carbazole derivatives for blue organic light-emitting diodes. Synth Met 2015; 203: 174-9.

[18] Chiu TL, Chen HJ, Hsieh YH, Huang JJ, Leung MK. High-efficiency blue phosphorescence organic light-Emitting diode with ambipolar carbazole triazole host. J Phys Chem C 2015; 119: 16846-52.

[19] Gaj MP, Fuentes-Hernandez C, Zhang Y, Marder S, Kippelen B. Highly efficient organic light-emitting diodes from thermally activated delayed fluorescence using a sulfone-carbazole host material. Org Electron 2015; 16: 109-12.

[20] Gao Z, Wang ZM, Shan T, Liu YL, Shen FZ, Pan YY, et al. High-efficiency deep blue fluorescent emitters based on phenanthro[9,10-d]imidazole substituted carbazole and their applications in organic light emitting diodes. Org Electron 2014; 15: 2667-76.

[21] Hong M, Ravva MK, Winget P, Brédas JL. Effect of substituents on the electronic structure and degradation process in carbazole derivatives for blue OLED host materials. Chem Mater 2016; 28: 5791-8.

[22] Yang XL, Xu XB, Zhou GJ. Recent advances of the emitters for high performance deep-blue organic light-emitting diodes. J Mater Chem C 2015; 3: 913-44.

[23] Sekine C, Tsubata Y, Yamada T, Kitano M, Doi S. Recent progress of high performance polymer OLED and OPV materials for organic printed electronics. Sci Technol Adv Mater 2016; 15: 034203.

[24] Minaev B, Baryshnikov G, Agren H. Principles of phosphorescent organic light emitting devices. Phys Chem Chem Phys 2014;16:1719-58.

[25] Guo X, Baumgarten M, Müllen K. Designing π-conjugated polymers for organic electronics. Prog Polym Sci 2013; 38: 1832-908.

[26] Singh G, Bhalla V, Kumar M. Carbazole end-capped and triphenylamine-centered starburst derivative for hole-transport in electroluminescent devices. Opt Mater 2015; 46: 82-7.

[27] Chen SF, Tian Y, Peng JH, Zhang HR, Feng XJ, Zhang HX, et al. Synthesis and characterization of arylamino end-capped silafluorenes for blue to deep-blue organic light-emitting diodes (OLEDs). J Mater Chem C 2015; 3: 6822-30.

[28] Zhang ZH, Jiang W, Ban XX, Yang M, Ye SH, Huang B, et al. Solution-processed efficient deep-blue fluorescent organic light-emitting diodes based on novel 9,10-diphenyl-anthracene derivatives. RSC Adv 2015; 5: 29708-17.

[29] Fleetham TB, Huang L, Klimes K, Brooks J, Li J. Tetradentate Pt(II) complexes with 6-membered chelate rings: A new route for stable and efficient blue organic light emitting diodes. Chem Mater 2016; 28: 3276-82.

[30] Yook KS, Lee JY. Organic materials for deep blue phosphorescent organic light-emitting diodes. Adv Mater 2012; 24: 3169-90.

[31] Tao Y, Yang C, Qin JG. Organic host materials for phosphorescent organic light-emitting diodes. Chem Soc Rev 2011; 40: 2943-70.

[32] Cui LS, Dong SC, Liu Y, Li Q, Jiang ZQ, Liao LS. A simple systematic design of phenylcarbazole derivatives for host materials to high-efficiency phosphorescent organic light-emitting diodes. J Mater Chem C 2013; 1: 3967-75.

[33] Xu B, Sheibani E, Liu P, Zhang J, Tian H, Vlachopoulos N, et al. Carbazole-based hole-transport materials for efficient solid-state dye-sensitized solar cells and perovskite solar cells. Adv Mater 2014; 26: 6629-34.

[34] Jiang JX, Jiang CY, Yang W, Zhen HY, Huang F, Cao Y. High-efficiency electrophosphorescent fluorene-*alt*-carbazole copolymers N-grafted with cyclometalated Ir complexes. Macromol 2005; 38: 4072-80.

[35] Xu C, Wakamiya A, Yamaguchi S. Ladder oligo(p-phenylenevinylene)s with silicon and carbon bridges. J Am Chem Soc 2005; 127: 1638-9.

[36] Long C, Lu JD, Li A, Hu D, Liu FQ, Zhang QX. Adsorption of naphthalene onto the carbon adsorbent from waste ion exchange resin: equilibrium and kinetic characteristics. J Hazard Mater 2008; 150: 656-61.

[37] Liu DD, Wu ZS, Tian F, Ye BC, Tong YB. Synthesis of N and La co-doped TiO_2/AC photocatalyst by microwave irradiation for the photocatalytic degradation of naphthalene. J. Alloys Compd 2016; 676: 489-98.

[38] Sahana A, Banerjee A, Lohar S, Das S, Hauli I, Mukhopadhya SK, et al. Naphthalene based highly selective OFF-ON-OFF type fluorescent probe for Al^{3+} and NO^{2-} ions for living cell imaging at physiological pH. Inorg Chim Acta 2013; 398: 64-71.

[39] Ünal A, Eren B, Eren E. Investigation of the azo-hydrazone tautomeric equilibrium in an azo dye involving the naphthalene moiety by UV-vis spectroscopy and quantum chemistry. J Mol Struct 2013; 1049: 303-9.

[40] Gu L, Zhu NW, Guo HQ, Huang SQ, Lou ZY, Yuan HP. Adsorption and fenton-like degradation of naphthalene dye intermediate on sewage sludge derived porous carbon. J Hazard Mater 2013; 246-247: 145-53.

[41] Kim GW, Lampande R, Choe DC, Bae HW, Kwon JH. Efficient hole injection material for low operating voltage blue fluorescent organic light emitting diodes. Thin Solid Films 2015; 589: 105-10.

[42] Zhang L, Zhang YX, Hu Y, Shi XB, Jiang ZQ, Wang ZK, et al. Highly efficient blue phosphorescent organic light-emitting diodes employing a host material with small bandgap. ACS Appl Mater Interfaces 2016; 8: 16186-91.

[43] Bai Q, Liu H, Yao L, Shan T, Li JY, Gao Y, et al. Adjusting nitrogen atom orientations of pyridine ring in tetraphenylsilane-based hosts for highly efficient blue phosphorescent organic light-emitting devices. ACS Appl Mater Interfaces 2016; 8: 24793-802.

[44] Yin NH, Feng LH. A novel blue emission PLED material: Synthesis, photophysical and electrochemical properties. Dyes Pigm 2015; 117: 116-21.

[45] Feng LH, Liang F, Wang Y, Xu M, Wang XJ. A highly sensitive water-soluble system to sense glucose in aqueous solution. Org Biomol Chem 2011; 9: 2938-42.

[46] Zhu JR, Yin NH, Feng LH. Two non-doped blue emitters for electroluminescent devices: preparation, photophysics and electroluminescence. Dyes Pigm 2016; 132: 121-7.

[47] Becke AD. Density-functional thermochemistry. III. the role of exact exchange. J Chem Phys 1993; 98: 5648-52.

[48] Frisch MJ, Trucks GW, Schlegel HB, Scuseria GE, Robb MA, Cheeseman JR, Scalmani G, Barone V, Mennucci B, Petersson GA, Nakatsuji H, Caricato M, Li X, Hratchian HP et al. Gaussian 09, Revision B01, Gaussian Inc., Wallingford, CT 2010.

[49] Zhai JY, Pan T, Zhu JW, Xu YM, Chen J, Xie YJ, Qin Y. Boronic Acid Functionalized Boron Dipyrromethene Fluorescent Probes: Preparation, Characterization, and Saccharides Sensing Applications. Anal Chem 2012; 84: 10214-10220.

The figures and scheme captions

Scheme 1. The synthesis routes of monomer 1, 2 and compound MNBC.

Fig. 1 The UV-Vis absorption and fluorescence emission spectra of MNBC in $CHCl_3$.

Fig. 2 TGA thermogram of MNBC with a heating rate of 5 ^oC/min under nitrogen atmosphere.

Fig. 3 Cyclic voltammogram of MNBC and molecular orbital surfaces of the HOMO and LUMO for MNBC. The supporting electrolyte is 0.10 M Bu_4NClO_4 in acetonitrile and the scan rate is 0.10 V/s.

Fig. 4 Properties of the device with the MNBC emitter. a) the schematic diagram of the device (ITO/PEDOT:PSS/MNBC/CBP/TPB/LiF/Al); b) The electroluminescence spectra of MNBC in the device under different voltages; c) Plot of voltage versus luminance for blue-light emitting device; d) Plot of voltage versus current density for blue-light emitting device.

Scheme 1

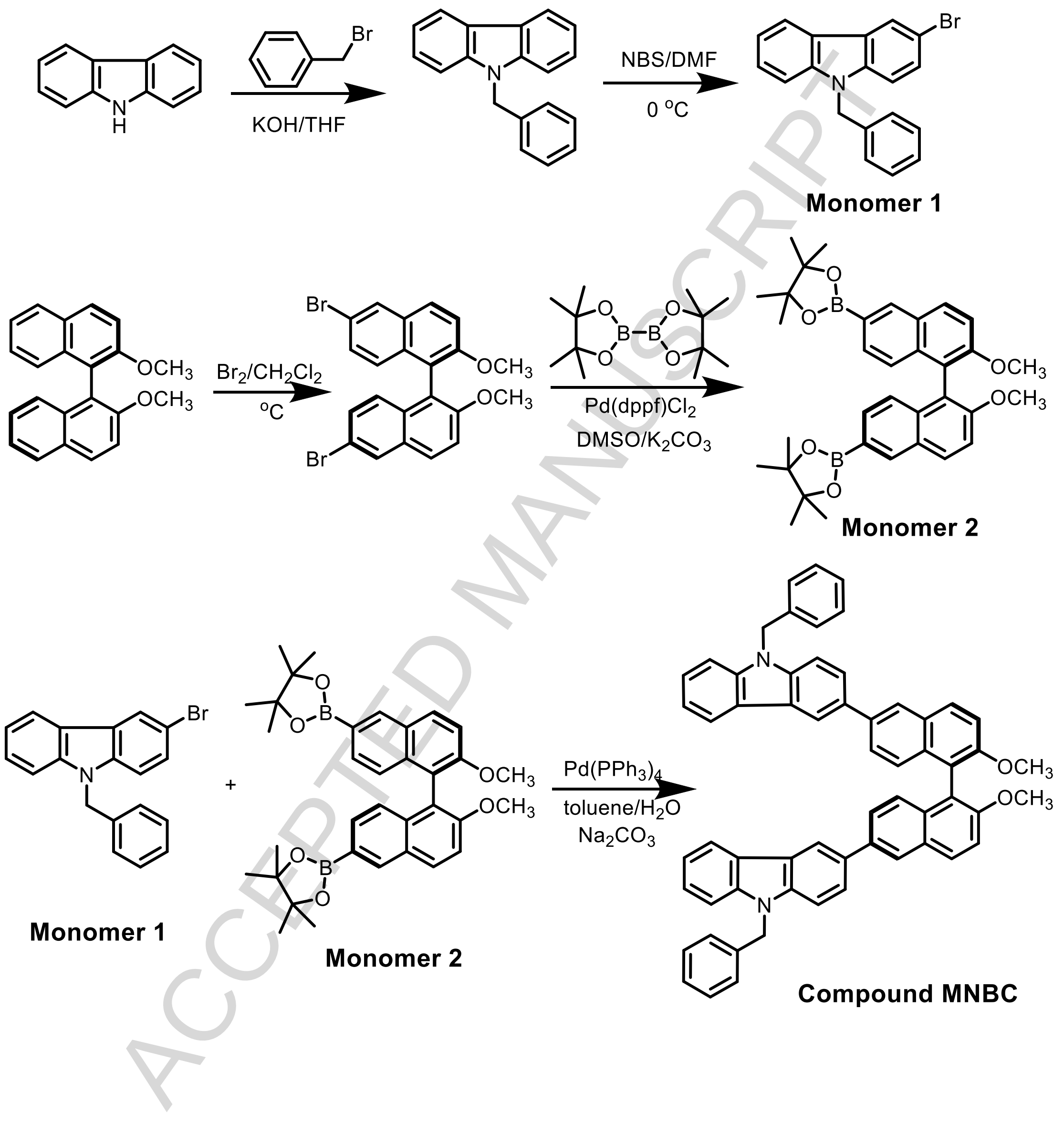
N
H
Br
KOH/THF
N
NBS/DMF
0 °C
Br
N
Monomer 1
OCH3
OCH3
Br2/CH2Cl2
°C
Br
Br
OCH3
OCH3
O
B
B
O
O
O
Pd(dppf)Cl2
DMSO/K2CO3
O
B
O
OCH3
OCH3
O
B
O
Monomer 2
Br
N
+
O
B
O
OCH3
OCH3
O
B
O
Monomer 1
Monomer 2
Pd(PPh3)4
toluene/H2O
Na2CO3
N
OCH3
OCH3
N
Compound MNBC

Fig. 1

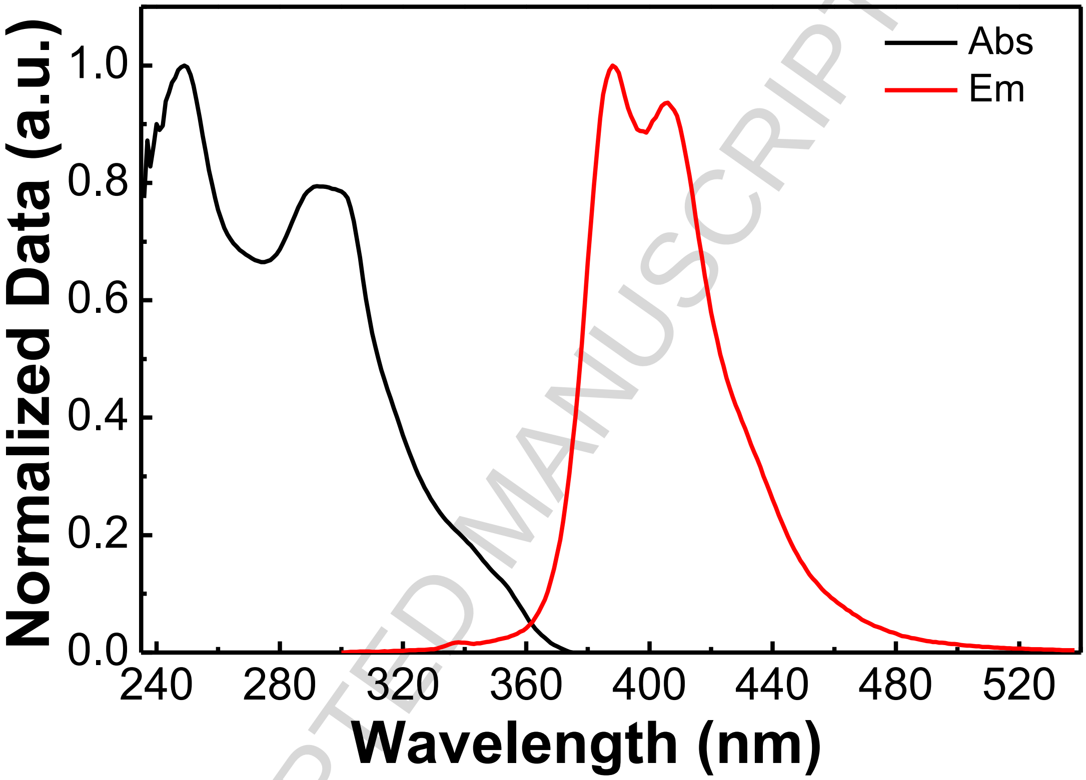
Abs
Em
Normalized Data (a.u.)
1.0
0.8
0.6
0.4
0.2
0.0
240
280
320
360
400
440
480
520
Wavelength (nm)

Fig. 2

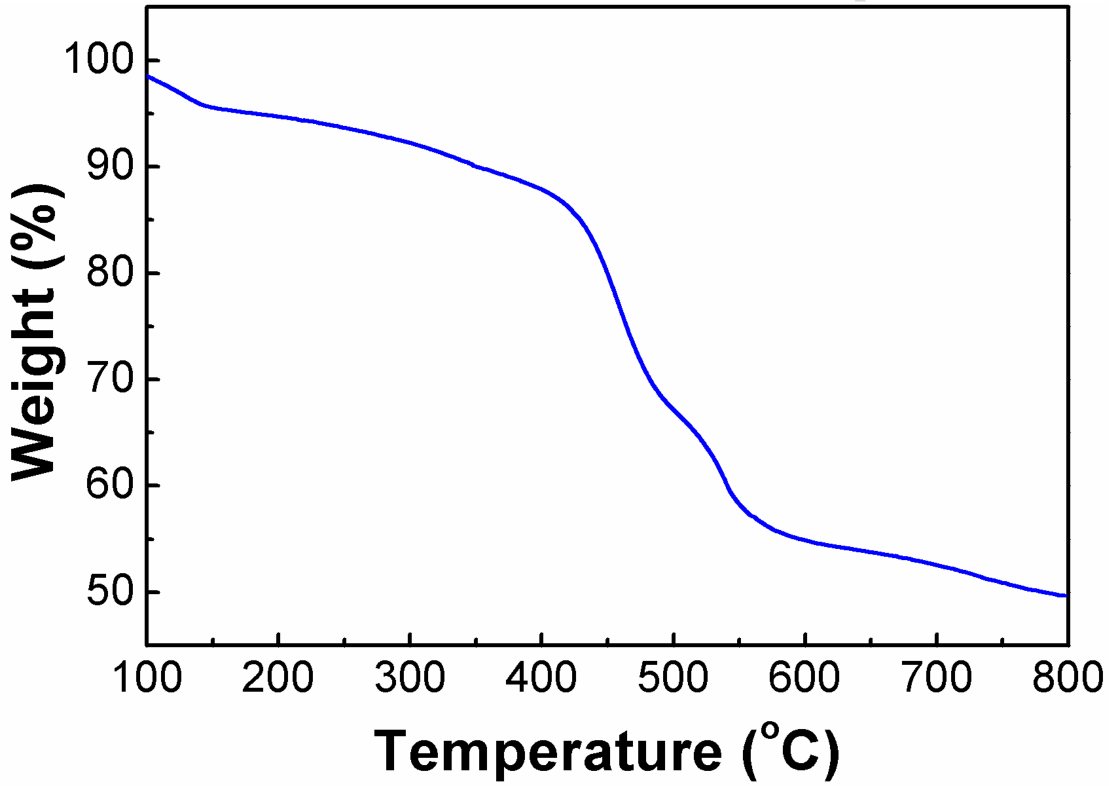
Weight (%)
100
90
80
70
60
50
100
200
300
400
500
600
700
800
Temperature (°C)

Fig. 3

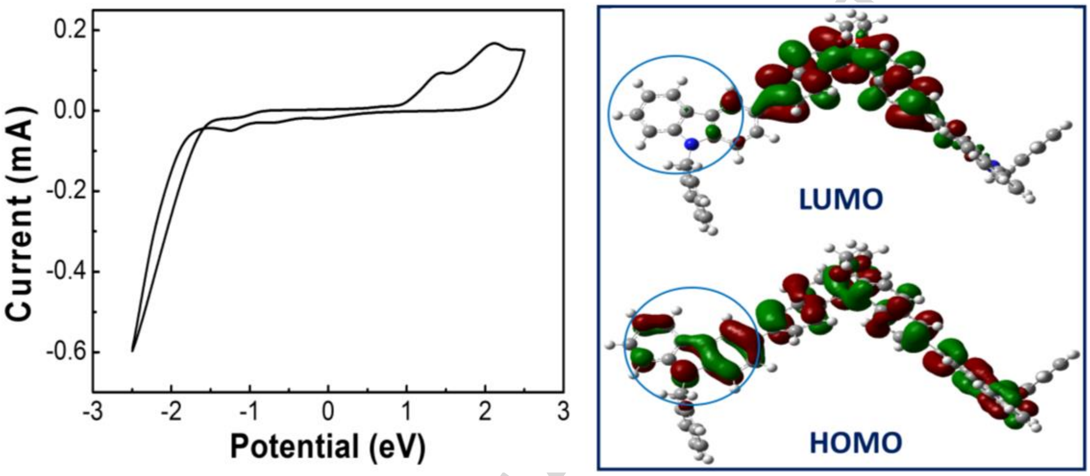

Fig. 4

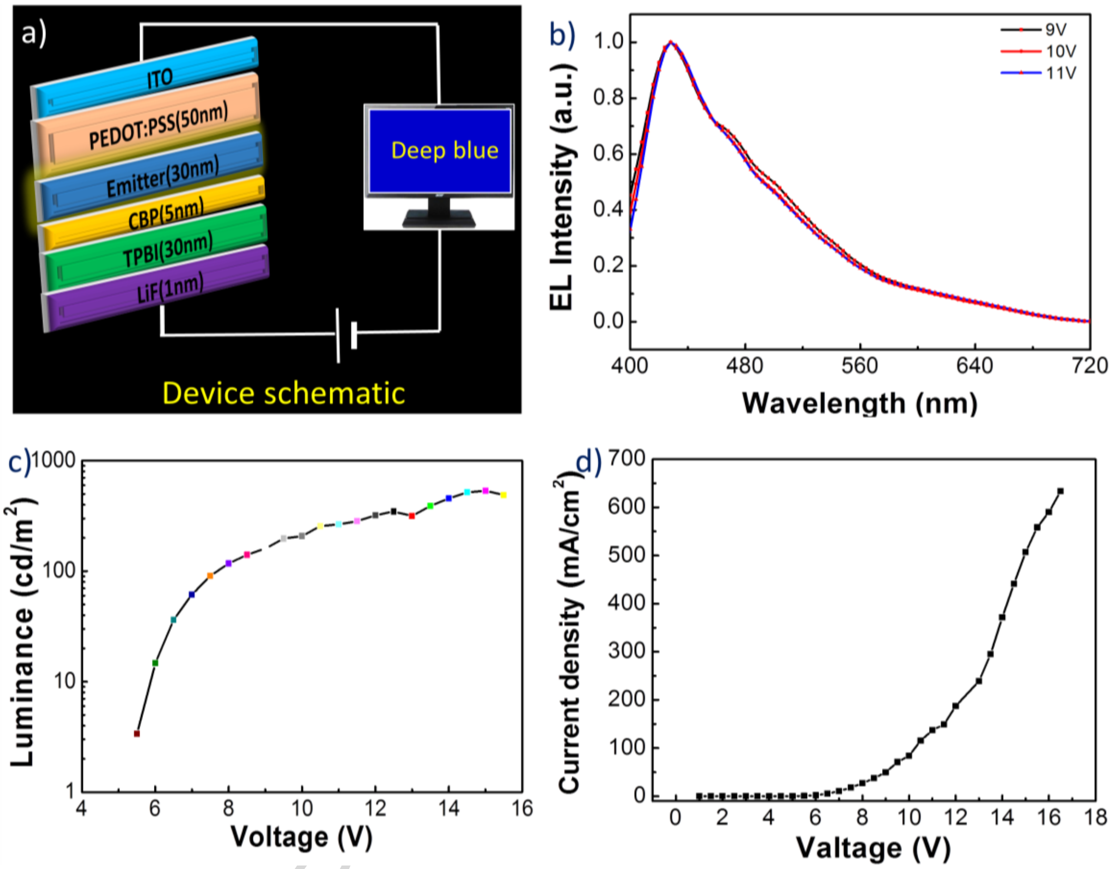
a)
ITO
PEDOT:PSS(50nm)
Emitter(30nm)
CBP(5nm)
TPBI(30nm)
LiF(1nm)
Deep blue
Device schematic
b)
EL Intensity (a.u.)
Wavelength (nm)
9V
10V
11V
0.0
0.2
0.4
0.6
0.8
1.0
400
480
560
640
720
c)
Luminance (cd/m^2)
Voltage (V)
1
10
100
1000
4
6
8
10
12
14
16
d)
Current density (mA/cm^2)
Valtage (V)
0
100
200
300
400
500
600
700
0
2
4
6
8
10
12
14
16
18

Graphical Abstract

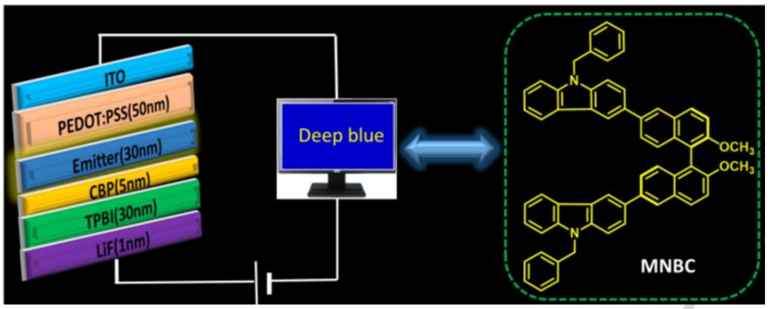

Highlights

A deep blue emitting OLED material was designed and prepared.

The emitter possesses good thermal stability and photophysical properties.

The device with the emitter exhibits good optical and electrical characteristics.